Non-Covalently Associated Streptavidin Multi-Arm Nanohubs Exhibit Mechanical and Thermal Stability in Cross-Linked Protein-Network Materials

David S. Knoff^{a,†}, Samuel Kim^{a,†}, Kareen A. Fajardo Cortes^a, Jocelyne Rivera^a, Marcus V. J. Cathey^a, Dallas Altamirano^a, Christopher Camp^a and Minkyu Kim^{a,b,c}*

^aDepartment of Biomedical Engineering, University of Arizona, Tucson, Arizona 85721

^bDepartment of Materials Science and Engineering, University of Arizona, Tucson, Arizona 85721

^cBIO5 Institute, University of Arizona, Tucson, Arizona 85719

Abstract

Constructing protein-network materials that exhibit physicochemical and mechanical properties of individual protein constituents requires molecular cross-linkers with specificity and stability. A well-known example involves specific chemical fusion of a four-arm polyethylene glycol (tetra-PEG) to desired proteins with secondary cross-linkers. However, it is necessary to investigate tetra-PEG like biomolecular cross-linkers that are genetically fused to the proteins, simplifying synthesis by removing additional conjugation and purification steps. Non-covalently, selfassociating, streptavidin homotetramer is a viable, biomolecular alternative to tetra-PEG. Here, a multi-arm streptavidin design is characterized as a protein-network material platform using various secondary, biomolecular cross-linkers, such as high-affinity physical (i.e., non-covalent), transient physical, spontaneous chemical (i.e., covalent), or stimuli-induced chemical cross-linkers. Stimuliinduced, chemical cross-linkers fused to multi-arm streptavidin nanohubs provide sufficient diffusion prior to initiating permanent covalent bonds, allowing proper characterization of streptavidin nanohubs. Surprisingly, non-covalently associated streptavidin nanohubs exhibit extreme stability which translates into material properties that resemble hydrogels formed by chemical bonds even at high temperatures. Therefore, this study not only establishes that the streptavidin nanohub is an ideal multi-arm biopolymer precursor but also provides valuable guidance for designing self-assembling nanostructured molecular networks that can properly harness the extraordinary properties of protein-based building blocks.

Keywords: Molecular self-assembly, protein cross-linkers, non-covalent interactions, artificial protein design, protein network, hydrogel.

Introduction

Functional proteins and molecular cross-linkers constitute protein-network materials, ubiquitous in nature, such as cytoskeleton¹⁻² and extracellular matrix.³⁻⁴ Understanding bulk physicochemical, biological, and single-molecule mechanical properties of functional proteins provides the opportunity to develop synthetic protein-network materials that mimic native biology for tissueengineered scaffolds,⁵ and further implement desired properties, such as resilience,⁶⁻⁷ passive elasticity of muscle, 8 strength, 9 and adhesion in aqueous environments. 10-11 Diverse synthetic and biological molecular cross-linkers are available to connect and exhibit physicochemical and biological properties of proteins in protein-network systems.^{7, 12-15} However, to exhibit bulk mechanical properties of protein-network materials, depending on constitutive mechanical proteins, selecting molecular cross-linkers requires more stringent conditions, such as specificity, functionality, and strength. 12 For instance, individual mechanical proteins exhibit their properties when external stresses stretch and unfold the protein via each terminus, 8, 15-18 necessitating high cross-linker specificity for crosslinking proteins end-to-end within the network. When crosslinkers are located at both termini of each protein, at least one cross-linker should have the functionality to connect with at least two other cross-linkers from separate functional proteins (f ≥ 3) to prepare a three-dimensional protein-network system. Furthermore, cross-linkers need to remain stable and intact to transmit the applied external stress across all protein strands in the protein network. Currently, such well-defined molecular cross-linkers that concurrently have high specificity and stability as well as the functionality within protein-network materials are limited.

A molecular cross-linker that meets these requirements is a four-arm polyethylene glycol (tetra-PEG)¹⁹ that has been chemically fused with specificity to proteins of interest with secondary cross-linkers at the other ends to form protein-network materials.¹² Tetra-PEG, which has a crosslinking functionality of four (f = 4), represents a trending strategy to develop star-like precursors that form polymer-network materials.^{12, 20-21} A major disadvantage of this approach to fabricate protein-network materials is the conjugation and purification steps required to chemically fuse tetra-PEG to proteins, which increases the complexity of synthesis and processing, and can reduce yields of the star-like precursors. This leads to the investigation of tetra-PEG-like protein cross-linkers that can be genetically fused to proteins of interest, simplifying multi-arm protein synthesis by bypassing the chemical conjugation and additional purification steps as well as improving the customizability and promoting the specific incorporation of functional proteins into strands of protein-network materials via genetic and protein engineering technology.²²

Secondary or tertiary structures of proteins self-recognize and non-covalently self-associate with each other, constituting quaternary or oligomeric structures that have been used as biomolecular cross-linkers. By genetically fusing the cross-linkers to proteins of interest using the

recombinant DNA technology, biosynthesized artificial proteins can construct predictable macromolecular structures, $^{23-26}$ such as multi-arm star-like precursors similar to tetra-PEG cross-linkers ($f \ge 3$). Furthermore, this approach enables the fabrication of protein-network materials with cross-linkers containing tailored binding affinity, modulating the intrinsic nature of protein associations and strands with customized length and mechanics. Despite these findings, the lack of cross-linker stability due to non-covalent interactions requires the investigation of strong and specific biomolecular cross-linkers to serve as multi-arm precursors that produce stable protein-network materials.

Well-known for having the strongest non-covalent interactions in nature with its ligand, biotin ($K_d = 10^{-14} \sim 10^{-16}$ M), $^{32-33}$ streptavidin (SAv) has been investigated for diverse biotechnology applications, 34 including binding assays, and purification strategies. Moreover, bulk biochemical study recognized that SAv forms thermally stable tetramers that can resist heat up to 75 °C and chemically stable against protein denaturants, such as 6 M GuHCl. 35 It is also identified that SAv tetramers are mechanically stable, specifically at the monomer-monomer interface where an AFM-based single-molecular force-spectroscopy study showed that this interface is four times stronger than the dimer-dimer interface. 23 Furthermore, these information has been the foundation to develop stable and precise nano-assemblies by applying the concept that SAv monomers naturally self-assemble into homotetramers with high affinity. 36 This indicates that SAv can be a viable strong and specific biomolecular cross-linker. When genetically fusing proteins of interest to one end of SAv monomers, biosynthesized artificial proteins will self-recognize and self-associate into a stable four-arm star-like precursor (f = 4), tetra-SAv (**Figure 1**).

One distinct advantage of using SAv as a cross-linker is its ability to orthogonally control material properties. Beyond the tetra-SAv, we can go further by genetically fusing proteins of interest on both ends of SAv monomers, where the biosynthesized proteins will self-assemble into an eight-arm precursor (f=8), octa-SAv. In addition, this molecular self-assembly approach still did not occupy the biotin binding site located in each SAv monomer, providing a mechanism for customizing octa-SAv precursors with the immobilization of biotinylated (macro)molecules, increasing up to 12 arm projections from an individual SAv cross-linker ($8 \le f \le 12$). Using the recombinant protein technology to incorporate mechanical proteins as SAv arms that can form protein-network materials and attach biochemical (macro)molecules via biotinylation, will achieve the orthogonal control of mechanical and biochemical properties of the materials.

While the specificity and stability, as well as ligand-receptor property, of SAv open these possibilities to be used as multi-arm molecular nanohubs, the tetramer itself has not been used as a cross-linking mechanism to fabricate protein-network materials. Thus, whether the SAv stability at the molecular level can be transferrable to the bulk material level is unknown.

Here, we investigated the feasibility of using tetra-SAv as a protein-based alternative to tetra-PEG in the formation of protein-network hydrogels. To construct hydrogels, tetra-SAv-based nanomolecular building blocks were designed by the genetic fusion of a SAv monomer and a panel of biomolecular cross-linkers on either ends of well-characterized non-structured proteins (Figure 1). Four classes of biomolecular cross-linkers, such as SAv, coiled-coil, SpyTag-SpyCatcher, and dityrosine, were chosen to study the hierarchical network formation of four-arm SAv precursors. Unlike SAv, each type has already been used to prepare protein-based hydrogels^{8, 15, 27} and can be categorized as stable physical (i.e., non-covalent), transient (or weak) physical, specific and spontaneous chemical (e.g., covalent), and stimuli-induced chemical cross-linkers, respectively (Figure 1). The variability of the biomolecular cross-linkers enabled an accurate characterization of SAv cross-linkers, where non-covalently associated SAv cross-linkers in protein-network materials are stable and behave like chemical bonds with specificity. Simultaneously, the systematic analysis of nanomolecular building blocks from the bottom-up design of proteinnetwork materials informs that the enhanced distribution of the building blocks within the network can be promoted by selecting the proper class of the secondary cross-linker. This, in turn, is crucial to reduce inhomogeneous crosslinking density and improve bulk mechanical properties of the protein-network material.³⁷⁻³⁸ Collectively, the presented protein-network design that allows precise characterization of SAv cross-linkers provides protein assembly strategies for incorporating functionality, specificity, binding strength, and kinetics of cross-linkers to optimize the material performances. Furthermore, this design approach is expected to impact the development of customizable material systems for diverse biotechnological applications, ranging from a synthetic scaffold that precisely mimics the extracellular microenvironment for tissue engineering³⁹⁻⁴⁰ to electronic implantables.⁴¹

Experimental Section

Protein Expression and Purification. Target genes were cloned, expressed, and purified according to methods described in the referenced article.³⁸ All gene sequences are described in the Supporting Information (**Table S1**). Each protein construct has SAv at the C-terminus to prevent the formation of inclusion bodies.^{23, 42} A₂YA₂-A₄₈-SAv was purified using inverse transition cycling (ITC), exploiting the lower critical solution temperature (LCST) of elastin-like polypeptides (ELPs).⁴³⁻⁴⁴ After four cycles of ITC purification,⁴⁴ samples were dialyzed in deionized water to remove all salt impurities. All purified protein samples were flash frozen using liquid nitrogen, lyophilized, and stored at -20 °C.

Physical Hydrogel Fabrication. Protein-based hydrogels with only physical cross-linkers, such as pentameric (P) coiled-coil and SAv, were prepared by hydrating lyophilized protein to 10% w/v in 20 mM tris buffer at pH 8.0.

SpyTag-SpyCatcher Heterodimer Formation. Spy-C₂₄-SAv hydrogels were prepared by hydrating lyophilized SpyTag-C₂₄-SAv and SpyCatcher-C₂₄-SAv proteins to 10% w/v, separately, in 20 mM tris buffer at pH 8.0, then mixing them at a 1:1 M ratio.

Photo-Cross-Linking. Lyophilized A_2YA_2 - A_{48} -SAv proteins were dissolved in 20 mM tris buffer while incubating on a rocker at 4°C for approximately 1 hr. Ammonium persulfate and tris(2,2′-bipyridyl)ruthenium(II) chloride hexahydrate (Sigma-Aldrich, St. Louis, MO, USA) were dissolved in 20 mM tris and added to the protein solution for a final concentration of 15 or 80 mM and 31 or 250 μ M, respectively, with 10% w/v A_2YA_2 - A_{48} -SAv. Hydrogels were prepared in a 4°C cold room by pipetting the mixture into a 14 mm diameter x 2 mm height mold and crosslinking 10 inches under a 24 W, 14×14 LED array emitting 460 nm blue light for 10 min. During photo-cross-linking, tris(2,2'-bipyridyl)ruthenium(II) ([Ru(II)bpy₃]²⁺) oxidation of the tyrosyl phenyl groups form a spontaneous chemical bond, consuming a persulfate anion. Once completed, hydrogels were cut to an 8 mm diameter to match the rheometer geometry.

Rheology. The viscoelastic mechanical properties were characterized using small amplitude oscillatory shear rheology on a Discovery Hybrid Rheometer 2 (TA Instruments, New Castle, DE, USA) with a sandblasted 20 mm cone-and-plate geometry at a 1° angle for physical secondary cross-linkers or a sandblasted 8 mm parallel plate geometry for chemical secondary cross-linkers and a sandblasted stage. Inertia, friction, and rotational mapping calibrations were performed prior to each experiment. A Peltier temperature-controlled stage maintained 25 °C for all rheology testing, except during temperature sweeps. Hydrogels with physical secondary cross-linkers were transferred to the stage and the geometry was lowered to the trim gap height of 55 µm. Excess gel was removed from the edges of the geometry before lowering it to the testing gap height at 50 µm. Hydrogels with chemical secondary cross-linkers were pre-cut and loaded to an axial force of 0.05 N. To control evaporation, a mineral oil barrier was placed around the edges of the geometry and the geometry was encased in a solvent trap with a water seal. Hydrogels relaxed for 1 hour prior to experimentation. Strain sweeps were performed from 0.01 to 1000% shear strain at a constant 10 rad s⁻¹ angular frequency. Frequency sweeps were performed from 0.01 to 100 rad s⁻¹ at a constant 1% shear strain, within the linear region of the strain sweep. Depending on the type of hydrogel, temperature sweeps were performed between 5°C to 95°C, inclusively, at a constant 10 rad s⁻¹ angular frequency and 1% shear strain, within the linear region of the strain sweep.

UV-Vis Temperature Sweep/Spectra. For ELP-SAv and only SAv proteins, absorbance at 350 nm were collected using a Cary 60 UV-vis spectrophotometer from 10 to 95 °C using a Peltier temperature controller with an equilibration time of 5 minutes. Absorbance spectra of SAv protein was collected between 270 and 800 nm at 25 °C (**Figure S1**).

Statistical Data Analysis. No data pre-processing or exclusion of outliers were applied when using Excel for statistical analysis. Rheology data sets pertaining to each hypothesis were analyzed using two-sided, independent samples t-tests to compare protein groups with a 0.01 threshold of significance. The sample size (N) for all experiments was N = 3, except for the Spy-C₂₄-SAv system (N = 4). P-values for all t test results were less than 0.01 and reported in the manuscript. All results written throughout the manuscript represent the mean \pm standard deviation, unless otherwise noted.

Theoretical Calculations. The theoretical shear elastic modulus (G') of biopolymers was calculated using the affine and phantom network models (**Table S2**), according to methods described in detail in the referenced articles.^{20, 38}

Results and Discussion

Artificial Protein with Tetra-SAv Cross-Linkers. To analyze the properties of proteinnetwork materials composed of tetra-SAv cross-linkers, we designed an artificial protein containing a SAv monomer on each end connected by an intrinsically disordered, flexible, polyelectrolyte-like protein containing 24 repeats of AGAGAGPEG amino acid sequence, denoted as C₂₄, ^{27, 38} which resulted in SAv-C₂₄-SAv proteins (Table S1). We expected that SAv monomers in SAv-C₂₄-SAv proteins would self-recognize and self-associate to form SAv homotetramers in aqueous buffer and develop hydrogels, similar to other well-known, non-covalently associating protein hydrogels. 14, 27, 38 However, failed attempts to fabricate SAv-C₂₄-SAv hydrogels between 10 – 20 w/v% led to an investigation of the binding mechanics. Here, we compared results of sodium dodecyl sulfate-polyacrylamide gel electrophoresis (SDS-PAGE) between SAv-C₂₄-SAv samples that were denatured into individual, unstructured proteins by boiling at 100°C and samples that were not boiled (Figure 2a) as it is known that unboiled SAv maintain its tetramer structures and are observed in SDS-PAGE. 45 Based on the two-fold difference in molecular weight between the boiled and unboiled conditions as well as the lack of bands at higher molecular weights in unboiled samples on the SDS-PAGE, we deduced that only two SAv-C₂₄-SAv proteins are interacting to form tetramers without higher order binding that would indicate protein-network formation. The close proximity of two SAv cross-linkers connected by a flexible C24 strand allowed SAv on the N- and C-terminus to bind within each individual protein, forming a self-loop with the high specificity and affinity⁴⁶⁻⁴⁷ (Figure 2b). Subsequently, two self-looped SAv-C₂₄-SAv proteins interact with each other to form a tetrameric SAv complex. This binding sequence explains the lack of gelation and highlights the difficulty of forming hydrogels with cross-linkers that have high affinity and specificity connected by a flexible strand in an A-B-A triblock configuration.

To prevent self-looping, we switched from the A-B-A polymer design, where streptavidin monomers are on both termini of the unstructured protein, to an A-B-C triblock configuration, where we limited our artificial protein designs to a single SAv cross-linker at the C-terminus and other physical or chemical crosslinking mechanisms at the N-terminus (Figure 1). With this design, SAv monomers form four-arm SAv precursors similar to the well-investigated tetra-PEG, ^{19, 21, 48} can be engineered to initiate gelation, and exhibit mechanical stability with the help of the secondary cross-linkers. For the secondary crosslinking method, we initially considered typical protein chemical crosslinking technique that forms covalent bonds between chemical groups, such as amine and carboxyl groups, on either end of protein strands. Although strong and stable, these chemical bonds generate random crosslinking junctions because of the prevalence of chemical groups in the side chains of protein structures incorporated into network strands. The lack of the crosslinking specificity loses the control over key parameters that affect the mechanical properties of protein-network materials, such as chain length and network topology.³⁷ To improve the specificity of this conventional chemical crosslinking strategy, molecular recognition (i.e., specificity) has developed prior to forming chemical bonds. ^{15, 25, 36, 49-50}

SAv-Based Protein-Network Hydrogels with Secondary, Specific, Spontaneous, Chemical Cross-Linkers. To apply the specific chemical crosslinking strategy, we implemented SpyTag-SpyCatcher chemistry, well-known for its ability to form spontaneous covalent isopeptide linkages between Asp117 of the SpyTag peptide and Lys31 of the SpyCatcher protein after the molecular recognition between those two molecules.⁴⁹ We genetically incorporated either SpyTag or SpyCatcher into the N-terminus of C₂₄-SAv and biosynthesized designed proteins (**Figure 3a-b**; **Figure S2**; Table S1). When mixing the solutions that contains either SpyTag-C₂₄-SAv or SpyCatcher-C₂₄-SAv, we observed a partially gelated slurry with dense gel formation where the two samples first interacted. However, a significant portion of the sample remains in liquid states due to the limited control of adequate mixing.⁵¹ This suggests that spontaneous cross-linking is susceptible to fabricating inhomogeneous protein-network materials. Protein— or polymernetwork inhomogeneity is a debilitating issue in the field, diminishing mechanical properties due to inefficient gelation kinetics and requiring fabrication techniques that improve the homogeneity of the mixture during the network formation.^{37, 51}

These qualitative observations were reflected in the rheological characterization (Figure 3c). Small amplitude oscillatory shear rheology captured the fast initial gelation from the Spy-C₂₄-SAv network (Figure S2), where Spy represents the linkage between SpyTag and SpyCatcher. However, the material is relatively weak at less than 100 Pa of shear elastic modulus (G'; $0.02 \pm 0.01 \text{ kPa}$; N=4). This measurement is within the 500 Pa range from prior studies that developed hydrogels using other SpyTag-SpyCatcher design strategies. ^{15, 50} However, this G' is weak relative

to other protein-network materials with similar molecular weight and is significantly lower than the predicted G' based on the polymer-network models^{20, 38} (Table S2). The experimental G' is approximately 1% of the theoretical G' from the affine and phantom polymer network models. Compared to other hydrogels in this study, the observed gelation indicates that the specific and spontaneous covalent bonds seem to initiate protein-network formation prior to adequate diffusion of protein building blocks, resulting in an inhomogeneous crosslinking density within the protein network (Figure 3d) along with other topological defects (e.g., high-order loops) that limits the ability to characterize the mechanical properties of SAv cross-linkers.

SAv-Based Protein-Network Hydrogels with Secondary, Transient Cross-Linkers. In addition to the specificity of biomolecular cross-linkers, their binding kinetics, dependent upon their binding affinity of non-covalent interactions,⁵² provide the ability to restructure the protein network and improve homogeneously distributed protein building blocks. 53-54 Biosynthetic coiledcoil protein structures, inspired by a variety of innate proteins such as cartilage oligomeric matrix protein and troponin, have been utilized as cross-linkers for the development of protein-network hydrogels with customizable network properties. 27-28, 38, 53-54 Coiled-coil cross-linkers, where multiple a-helical structures physically inter-wound each other, undergo transient binding kinetics where cross-linkers can bind and unbind periodically. These temporary bonds promote proteinnetwork homogeneity by allowing protein building blocks to diffuse throughout the hydrogel over time. 52-54 This ability to reorganize protein networks presented a viable option for improving network homogeneity in our tetra SAv-based protein-network design, engineering a monomer of pentameric coiled-coil cross-linker (P) at the N-terminus to form P-C₂₄-SAv (Figure 4a; Table S1). SAv monomers in each protein led to form SAv tetramers with four protein arms (Figure 4a) due to their high affinity^{23, 35} as we confirmed on the SDS-PAGE⁴⁵ (Figure 4d). Then, transient P cross-linkers are expected to construct protein-network hydrogels (Figure 4b). Upon adding physiological buffer, the artificial protein with 10 w/v% formed a hydrogel with good qualitative uniformity (Figure 4c), compared to the partial gelation of the Spy-C₂₄-SAv spontaneous crosslinking system, and showed no signs of protein aggregation as the hydrogel is optically transparent. During SDS-PAGE analysis (Figure 2 and Figure 4d), we noticed that the protein samples ran slowly, which is caused by C₂₄ as it was already reported by our previous work.³⁸ We further confirmed its molecular weight using liquid chromatography-mass spectrometry (Figure S3). Characterizing the mechanical properties using rheology, we measured G' of P-C₂₄-SAv gels to be 1.6 \pm 0.1 kPa (N=3; Figure 4e), a significant improvement compared to the Spy-C₂₄-SAv hydrogels (0.02 \pm 0.01 kPa; N=4; p < 0.01; see the Experimental Section). Also, the effective crosslinking density is improved from ~1% to 26% and 47% when comparing the experimental G' to the affine and phantom polymer network models (Table S2). While there is an improvement in

the experimental G', it is difficult to make a direct comparison between these two hydrogels due to a difference in functionality between SpyCatcher-SpyTag (f = 2) and P cross-linker (f = 5). For example, there is a 38.5% decrease in G' compared to a prior study that developed physical hydrogels using P cross-linkers on both ends of $C_{24} (2.6 \pm 0.4 \text{ kPa})^{38}$. Since SAv has a different functionality (f = 4) compared to a P cross-linker (f = 5), this potentially results in the difference in G'. Therefore, the experimental G' was compared with the theoretical G' from affine and phantom polymer network models.

Even though the increase in G' (Figure 4b) can correlate to improvements in the overall mechanical properties, P-C₂₄-SAv hydrogel still lacked enough stability to characterize the properties of SAv cross-linkers. SAv tetramers are known to exhibit robust thermal stability that prevent their denaturation at temperatures up to approximately 85 °C.35 During the rheological characterization of P-C₂₄-SAv hydrogel, we increased the temperature to investigate whether this thermal stability of SAv tetramers translates into the bulk mechanical properties. G' decreased by $93.9 \pm 5.4 \%$ (N=3) at 60 °C compared to 25 °C (Figure 4f). This could be due to the transient kinetics of P cross-linkers where higher temperatures promote the dissociation of coiled-coil structures. 53-55 However, it also cannot be excluded that the G' drop can be due to the dissociation of non-covalently associated SAv homotetramers in the bulk hydrogel. Overall, the specific and transient physical associations of coiled-coil cross-linkers are beneficial because the transient kinetics can increase the building block homogeneity within protein networks (Figure 4d) compared to the specific and spontaneous covalent bonds of SpyTag-SpyCatcher cross-linkers (Figure 3). However, to adequately characterize the properties of tetra-SAv in protein-network hydrogels, the secondary crosslinking mechanism requires stability that exceeds the mechanical strength of SAv tetramers, in addition to the specificity and controlled binding kinetics.

Mechanical and Thermal Stabilities of Tetra-SAv Cross-Linkers in Protein-Network Hydrogels with Secondary, Stimuli-Induced, Chemical Cross-Linkers. Dityrosine photo-initiated chemical crosslinking can be the proper secondary crosslinking method because proteins with tyrosine residues can diffuse in solution prior to the formation of dityrosine covalent bonding between the tyrosine residues by blue-light irradiation. To avoid unintended dityrosine chemical crosslinking, the flexible C₂₄ chain, which contains uncontrolled tyrosine residues, was replaced by ELP with a similar number of amino acid residues to C₂₄ (Table S1). ELP has been extensively studied for its biocompatible and stimuli responsive properties for biomaterial applications. ⁵⁶⁻⁵⁷ It is also well-known for simple and effective purification of target proteins when genetically fused to ELP, using its temperature-responsive phase transition in solution. ⁴³ In our previous study, we used ELP with controlled numbers of tyrosine residues to modulate mechanical properties in photo-crosslinked protein-network materials. ⁴⁴ We adapted the ELP sequence and further

engineered to prepare A_2YA_2 - A_{48} -SAv artificial proteins (**Figure 5a**), where A and Y represent the five amino acid sequence, VPGXG with either alanine (A) and tyrosine (Y) in the X position, respectively. Thereby, offering only one site of photo-crosslinking at the end of each ELP arm, which is at the opposite terminus to the SAv physical cross-linkers (Figure 5a; Table S1).

The A₂YA₂-A₄₈-SAv protein design successfully combined dityrosine chemical crosslinking and SAv physical crosslinking. The experimental G' of the hydrogel, composed of four-arm SAv precursors with secondary dityrosine photo-crosslinking (Figure 5a-b), is 2.8 ± 0.4 kPa (N=3), which had an approximately 700-fold increase compared to the G' of the Spy-C₂₄-SAv hydrogel (p < 0.01; Figure 3c). In addition, the experimental G' is approximately 70% of the theoretical G' from the affine network model (Table S2). The experimental G' was expected to be lower than the theoretical G' since it is well-known that there are topological defects, such as selfloops and dangling chains, in polymer/protein networks with flexible strands. 20, 37-38 However, we see a significant improvement in hydrogel fabrication and G' when replacing the SpyTag-SpyCatcher mechanism (f = 2) to a more controllable dityrosine photo-crosslinking (f = 2). This confirms that controlling the secondary crosslinking allows enough time for these cross-linkers to diffuse throughout the protein network before permanent chemical bond formation, which is crucial in improving mechanical properties or effective junctions in the network. Furthermore, we compared the experimental G' of A₂YA₂-A₄₈-SAv to prior studies that characterized covalently crosslinked tetra-PEG hydrogels (i.e., synthetic counterpart of SAv tetramer). Despite the similar functionality between dityrosine photo-crosslinking and other covalent crosslinking mechanisms used in prior studies (f = 2), the experimental G' is significantly different from covalently crosslinked tetra-PEG hydrogels where the experimental G' ranges from 0.2 to 200 kPa due to several factors, such as numbers of cross-linkers, polymer concentrations, and chain length/mesh sizes. 58-61

Similar to covalently crosslinked tetra-PEG hydrogels from prior studies, the G' of A₂YA₂-A₄₈-SAv hydrogel did not show the same frequency dependency as P-C₂₄-SAv (Figure 4e), where G' is dominating over G" even at low frequencies despite the physical interactions of SAv tetramers (Figure 5c). This indicates that the reason why the P-C₂₄-SAv acts like a physical gel, where the G' of P-C₂₄-SAv is frequency dependent, is because of the P cross-linker (Figure 4b). In contrast, the dityrosine photo-crosslinking mechanism causes the A₂YA₂-A₄₈-SAv hydrogel to behave like a chemically crosslinked hydrogel although SAv tetramers are physically associated. Therefore, we confirm that SAv is a mechanically stable cross-linker with high specificity.

A caveat of dityrosine chemical crosslinking in protein-network materials is the limited control of the specificity in crosslinking when incorporating natural proteins where their structures require Tyr residues. Although we controlled the location and number of Tyr residues in the ELP sequence (Figure 5a), the SAv sequence contains Tyr residues that cannot be removed without

possibly compromising its structure. These Tyr residues could generate unintentional SAv-A₂YA₂ or SAv-SAv dityrosine chemical crosslinking, potentially explaining the lack of frequency dependency in a non-covalently associated physical hydrogel (Figure 5c) and the experimental G' approximately 140% of the theoretical G' from the phantom network model²⁰ (Table S2). However, there is a possibility that this unintentional dityrosine chemical crosslinking does not affect the crosslinking mechanism of SAv. The dimer-dimer interface of SAv homotetramers is the location where the SAv cross-linker will break by the external stress since that interface is weaker than the monomer-monomer interface.^{23, 35} In the case of SAv-A₂YA₂ crosslinking, the single tyrosine at the end of the ELP cannot covalently bind at the dimer-dimer interface due to the absence of tyrosine residues in that region (**Figure S4**). Therefore, this should not affect the physical interaction at the weak dimer-dimer interface which supports the fact that the lack of frequency dependency is not caused by any SAv-A₂YA₂ crosslinking.

The possibility of SAv-SAv crosslinking for the lack of frequency dependency (Figure 5c) was determined using SDS-PAGE by evaluating whether tyrosine residues in SAv can introduce unspecific dityrosine crosslinking. We found that photo-crosslinked SAv tetramers at 10 w/v% can form unspecific dityrosine bonds with the photo-crosslinking reagents of 250 μ M ruthenium and 80 mM ammonium persulfate (**Figure S5**). However, the Tyr residues are not located at the dimerdimer interface of SAv tetramers based on molecular visualization (Figure S4). This suggests that the non-covalently associated dimer-dimer interface of SAv cross-linkers is still intact and can be dissected during rheology characterization. Since we did not see the physical behavior in hydrogel rheology, this indicates that the physically associated SAv tetramer behaves like a chemical cross-linker with the high specificity.

To confirm whether any SAv-SAv crosslinking affects the interfaces of SAv tetramers, we prepared the hydrogel with the reduced reagent concentration to 31μM ruthenium and 15mM ammonium persulfate which minimized unspecific crosslinking between SAv tetramers (Figure S5). While the reduced concentration impacted the G′ as expected based on our previous report on ELP gels, 44 the crossover frequency was still not observed (Figure 5d). In addition, we replaced the single Tyr in the ELP with a valine residue to determine whether the single Tyr in the ELP domain plays an important role in forming the hydrogel (Table S1; **Figure S6**). Here, we saw no signs of gelation when the ELP-SAv protein construct does not have the single Tyr residue in the ELP domain even though there are SAv-SAv crosslinking (Figure S6b). This indicates that this single Tyr in the ELP is significant in forming a hydrogel and SAv-SAv crosslinking alone cannot form a hydrogel. Therefore, we concluded that, due to the high mechanical stability, the specifically self-associated, tetra-SAv in protein-network hydrogel behaves like a chemical crosslinker despite the fact that tetra-SAv is formed from non-covalent interactions.

To correlate the thermal stability of SAv from bulk, biochemical measurements to tetra-SAv within protein-network materials, the temperature-dependence of SAv-based hydrogels was evaluated. In temperature sweep rheology, we identified that the G' of the hydrogel significantly increased at > 60°C (Figure 6a). This was caused by the incorporated ELP that has the LCST behavior at approximately 60 °C (Figure 6b) due to the phase separation or coacervation property of ELP which occur above certain temperature depending on ELP sequences. As we expected, this affect was shown in the changes of G' across temperatures, where the intersection of the trendlines correlates with the occurrence of the ELP coacervation (Figure 6a). In addition, this mechanical reinforcement was already observed by the other ELP-based material system.⁵⁷ When we further increase the temperature above the LCST and performed the frequency sweep experiment at 85°C (Figure 6c), we observed G' is greater than G" throughout angular frequencies below 10 rad/s where the crossover frequency (G' = G'') or fluid behavior (G'' > G') is generally present when characterizing physically-associated hydrogels (e.g., Figure 4e). Note that there were increases in the noise of the G" data, meaning that the measurements were susceptible due to the decrease in concentrations of photo-crosslinking reagents (Figure 5d and Figure S5) which lowers the associated effective crosslinking density. It is also possible that higher temperatures than the ELP LCST potentially impacted the G" (Figure 6c and Figure S5) due to the coacervation property of ELP. Nonetheless, we still clearly noticed that increasing temperature for Tyr-ELP-SAv hydrogel with low ruthenium and ammonium persulfate (Figure 5d) did not show the crossover frequency (Figure S7). As a result, the absence of a crossover frequency even at high temperatures and lower number of photo-crosslinked dityrosine bonds indicates that the SAv tetramer was not responsible for any shear-stimulated, dissociation of its crosslinking when complemented with a secondary, transient cross-linker (Figure 4e). Furthermore, the data indicate that the tetra-SAv in proteinnetwork materials is intact at the extreme temperature, confirming that tetra-SAv precursors are not only mechanically stable, but also thermally stable.

While we successfully characterized the stability of SAv nanohubs in protein-network hydrogels, we identified that the secondary cross-linking mechanisms are critical on the effective crosslinking density. Stimuli-induced chemical crosslinking mechanism can potentially overcome a few topological defects in protein networks, such as self-loops (Figure 2) and inhomogeneous protein-network formation (Figure 3). Still, this system cannot be free from other topological defects, such as dangling chains, and higher-order loops,³⁷ as experimental G' is reduced compared to theoretical G' (Figures 4-5; Table S2). By further modulating the flexibility of protein strands between biomolecular cross-linkers,³⁸ this challenge can be addressed.

Conclusions

Here, we investigated SAv tetramer as a stable and specific cross-linker for the development of protein-network materials or hydrogels. SAv was genetically engineered into artificial protein designs, resulting in individual proteins that self-recognize and self-associate with extreme affinity to form a four-arm tetramer hydrogel precursor. The systematic characterization of four-arm SAv-based hierarchical nanoassembly using a variety of second-level molecular self-assembly or specific chemical cross-linking methods discovered that stimuli-induced chemical cross-linkers, such as dityrosine photo-cross-linking, are optimal for developing protein-network materials with enhanced specificity, stability, and network homogeneity.

This customizable platform design can be engineered at the genetic level to incorporate target proteins with key mechanical, or biochemical properties in protein-network strands or investigate alternative stimuli-induced chemical cross-linkers, such as GB_1 , ²⁶ to further improve secondary crosslinking specificity. Moreover, biotinylated molecules can be orthogonally coordinated with the SAv-based protein-network system by using the strong protein-ligand interaction of SAv-biotin for diverse biomedical applications, such as advanced cell signaling, drug delivery, biosensing, and imaging. Therefore, SAv cross-linkers as the molecular nanohub will be the essential component of functional protein-network materials.

ASSOCIATED CONTENT

Supporting Information

The Supporting Information is available free of charge.

Illustrations of streptavidin tetramer with Tyr locations; Tyr crosslinking of SAv analyzed by SDS-PAGE; representative rheological characterization of protein hydrogels; full protein sequences; and theoretical shear elastic modulus predictions based on network models. (PDF)

AUTHOR INFORMATION

Corresponding Author

Minkyu Kim – Department of Biomedical Engineering, University of Arizona, Tucson, AZ 85721, USA; Department of Materials Science and Engineering, University of Arizona, Tucson, AZ 85721, USA; Bio5 Institute, University of Arizona, Tucson, AZ 85719, USA; Email: minkyukim@arizona.edu

Authors

- **David S. Knoff** Department of Biomedical Engineering, University of Arizona, Tucson, AZ 85721, USA
- **Samuel Kim** Department of Biomedical Engineering, University of Arizona, Tucson, AZ 85721, USA
- **Kareen A. Fajardo Cortes** Department of Biomedical Engineering, University of Arizona, Tucson, AZ 85721, USA
- **Jocelyne Rivera** Department of Biomedical Engineering, University of Arizona, Tucson, AZ 85721, USA
- Marcus V. J. Cathey Department of Biomedical Engineering, University of Arizona, Tucson, AZ 85721, USA
- **Dallas Altamirano** Department of Biomedical Engineering, University of Arizona, Tucson, AZ 85721, USA
- Christopher P. Camp Department of Biomedical Engineering, University of Arizona, Tucson, AZ 85721, USA

Author Contributions

† D.S.K. and S.K. contributed equally.

Notes

The authors declare no competing financial interests.

ACKNOWLEDGMENT

We are grateful for our support from the National Heart, Lung, and Blood Institute of the National Institutes of Health (T32HL007955; D.S.K.), the ARCS® Foundation (D.S.K.), the Louise Foucar Marshall Foundation (D.S.K.), the Department of Education Federal TRIO Programs (Grant #P217A170284; K.A.F.C. and D.A.), the NIH Maximizing Access to Research Careers grant (T34GM008718; J.R.), the NSF CAREER grant (DMR-2143126), and the Tech Launch Arizona at the University of Arizona. The content is solely the responsibility of the authors and does not necessarily represent the official views of the National Institutes of Health.

REFERENCES

- 1. Johnson, C. P.; Tang, H.-Y.; Carag, C.; Speicher, D. W.; Discher, D. E., Forced Unfolding of Proteins Within Cells. *Science* **2007**, *317* (5838), 663-666.
- 2. Fletcher, D. A.; Mullins, R. D., Cell mechanics and the cytoskeleton. *Nature* **2010**, *463* (7280), 485-492.
- 3. Engler, A. J.; Sen, S.; Sweeney, H. L.; Discher, D. E., Matrix Elasticity Directs Stem Cell Lineage Specification. *Cell* **2006**, *126* (4), 677-689.
- 4. Chaudhuri, O.; Cooper-White, J.; Janmey, P. A.; Mooney, D. J.; Shenoy, V. B., Effects of extracellular matrix viscoelasticity on cellular behaviour. *Nature* **2020**, *584* (7822), 535-546.
- 5. Wang, H.; Heilshorn, S. C., Adaptable Hydrogel Networks with Reversible Linkages for Tissue Engineering. *Adv. Mater.* **2015**, *27* (25), 3717-3736.
- 6. Elvin, C. M.; Carr, A. G.; Huson, M. G.; Maxwell, J. M.; Pearson, R. D.; Vuocolo, T.; Liyou, N. E.; Wong, D. C. C.; Merritt, D. J.; Dixon, N. E., Synthesis and properties of crosslinked recombinant pro-resilin. *Nature* **2005**, *437* (7061), 999-1002.
- 7. Liang, Y.; Li, L.; Scott, R. A.; Kiick, K. L., 50th Anniversary Perspective: Polymeric Biomaterials: Diverse Functions Enabled by Advances in Macromolecular Chemistry. *Macromolecules* **2017**, *50* (2), 483-502.
- 8. Lv, S.; Dudek, D. M.; Cao, Y.; Balamurali, M. M.; Gosline, J.; Li, H., Designed biomaterials to mimic the mechanical properties of muscles. *Nature* **2010**, *465* (7294), 69-73.
- 9. Ling, S.; Chen, W.; Fan, Y.; Zheng, K.; Jin, K.; Yu, H.; Buehler, M. J.; Kaplan, D. L., Biopolymer nanofibrils: Structure, modeling, preparation, and applications. *Prog. Polym. Sci.* **2018**, *85*, 1-56.
- 10. Waite, J. H., Mussel adhesion essential footwork. J. Exp. Biol. 2017, 220 (4), 517-530.
- 11. Deepankumar, K.; Lim, C.; Polte, I.; Zappone, B.; Labate, C.; De Santo, M. P.; Mohanram, H.; Palaniappan, A.; Hwang, D. S.; Miserez, A., Supramolecular β-Sheet Suckerin–Based Underwater Adhesives. *Adv. Funct. Mater.* **2020**, *30* (16), 1907534.
- 12. Wu, J.; Li, P.; Dong, C.; Jiang, H.; Bin, X.; Gao, X.; Qin, M.; Wang, W.; Bin, C.; Cao, Y., Rationally designed synthetic protein hydrogels with predictable mechanical properties. *Nat. Commun.* **2018**, *9* (1), 620.
- 13. Lu, H. D.; Wheeldon, I. R.; Banta, S., Catalytic biomaterials: engineering organophosphate hydrolase to form self-assembling enzymatic hydrogels. *Protein Eng., Des. Sel.* **2010,** *23* (7), 559-566.
- 14. Kim, M.; Chen, W. G.; Kang, J. W.; Glassman, M. J.; Ribbeck, K.; Olsen, B. D., Artificially Engineered Protein Hydrogels Adapted from the Nucleoporin Nsp1 for Selective Biomolecular Transport. *Adv. Mater.* **2015**, *27* (28), 4207-4212.

- 15. Sun, F.; Zhang, W.-B.; Mahdavi, A.; Arnold, F. H.; Tirrell, D. A., Synthesis of bioactive protein hydrogels by genetically encoded SpyTag-SpyCatcher chemistry. *Proc. Natl. Acad. Sci. U. S. A.* **2014**, *111* (31), 11269-11274.
- 16. Li, H.; Linke, W. A.; Oberhauser, A. F.; Carrion-Vazquez, M.; Kerkvliet, J. G.; Lu, H.; Marszalek, P. E.; Fernandez, J. M., Reverse engineering of the giant muscle protein titin. *Nature* **2002**, *418* (6901), 998-1002.
- 17. Lee, G.; Abdi, K.; Jiang, Y.; Michaely, P.; Bennett, V.; Marszalek, P. E., Nanospring behaviour of ankyrin repeats. *Nature* **2006**, *440* (7081), 246-249.
- 18. Rief, M.; Gautel, M.; Oesterhelt, F.; Fernandez, J. M.; Gaub, H. E., Reversible Unfolding of Individual Titin Immunoglobulin Domains by AFM. *Science* **1997**, *276* (5315), 1109-1112.
- 19. Sugimura, A.; Asai, M.; Matsunaga, T.; Akagi, Y.; Sakai, T.; Noguchi, H.; Shibayama, M., Mechanical properties of a polymer network of Tetra-PEG gel. *Polym. J.* **2013**, *45* (3), 300-306.
- 20. Zhong, M.; Wang, R.; Kawamoto, K.; Olsen, B. D.; Johnson, J. A., Quantifying the impact of molecular defects on polymer network elasticity. *Science* **2016**, *353* (6305), 1264-1268.
- 21. Sakai, T.; Matsunaga, T.; Yamamoto, Y.; Ito, C.; Yoshida, R.; Suzuki, S.; Sasaki, N.; Shibayama, M.; Chung, U.-i., Design and Fabrication of a High-Strength Hydrogel with Ideally Homogeneous Network Structure from Tetrahedron-like Macromonomers. *Macromolecules* **2008**, *41* (14), 5379-5384.
- 22. Yang, Y. J.; Holmberg, A. L.; Olsen, B. D., Artificially Engineered Protein Polymers. *Annu. Rev. Chem. Biomol. Eng.* **2017**, *8* (1), 549-575.
- 23. Kim, M.; Wang, C.-C.; Benedetti, F.; Rabbi, M.; Bennett, V.; Marszalek, P. E., Nanomechanics of Streptavidin Hubs for Molecular Materials. *Adv. Mater.* **2011**, *23* (47), 5684-5688.
- 24. Veggiani, G.; Nakamura, T.; Brenner, M. D.; Gayet, R. V.; Yan, J.; Robinson, C. V.; Howarth, M., Programmable polyproteams built using twin peptide superglues. *Proc. Natl. Acad. Sci. U. S. A.* **2016**, *113* (5), 1202-1207.
- 25. Zhang, W.-B.; Sun, F.; Tirrell, D. A.; Arnold, F. H., Controlling Macromolecular Topology with Genetically Encoded SpyTag–SpyCatcher Chemistry. *J. Am. Chem. Soc.* **2013**, *135* (37), 13988-13997.
- 26. Wang, R.; Li, J.; Li, X.; Guo, J.; Liu, J.; Li, H., Engineering protein polymers of ultrahigh molecular weight via supramolecular polymerization: towards mimicking the giant muscle protein titin. *Chem. Sci.* **2019**, *10* (40), 9277-9284.
- 27. Shen, W.; Zhang, K.; Kornfield, J. A.; Tirrell, D. A., Tuning the erosion rate of artificial protein hydrogels through control of network topology. *Nat. Mater.* **2006**, *5* (2), 153-158.

- 28. Lv, S.; Cao, Y.; Li, H., Tandem Modular Protein-Based Hydrogels Constructed Using a Novel Two-Component Approach. *Langmuir* **2012**, *28* (4), 2269-2274.
- 29. Dooling, L. J.; Tirrell, D. A., Engineering the Dynamic Properties of Protein Networks through Sequence Variation. *ACS Cent. Sci.* **2016**, *2* (11), 812-819.
- 30. Su, J. Y.; Hodges, R. S.; Kay, C. M., Effect of Chain Length on the Formation and Stability of Synthetic alpha-Helical Coiled Coils. *Biochemistry* **1994**, *33* (51), 15501-15510.
- 31. Wang, C.; Stewart, R. J.; KopeČek, J., Hybrid hydrogels assembled from synthetic polymers and coiled-coil protein domains. *Nature* **1999**, *397* (6718), 417-420.
- 32. Weber, P. C.; Ohlendorf, D. H.; Wendoloski, J. J.; Salemme, F. R., Structural Origins of High-Affinity Biotin Binding to Streptavidin. *Science* **1989**, *243* (4887), 85-88.
- 33. Reznik, G. O.; Vajda, S.; Smith, C. L.; Cantor, C. R.; Sano, T., Streptavidins with intersubunit crosslinks have enhanced stability. *Nat. Biotechnol.* **1996**, *14* (8), 1007-1011.
- 34. Dundas, C. M.; Demonte, D.; Park, S., Streptavidin–biotin technology: improvements and innovations in chemical and biological applications. *Appl. Microbiol. and Biotechnol.* **2013**, *97* (21), 9343-9353.
- 35. González, M. n.; Argaraña, C. E.; Fidelio, G. D., Extremely high thermal stability of streptavidin and avidin upon biotin binding. *Biomol. Eng.* **1999**, *16* (1), 67-72.
- 36. Fairhead, M.; Veggiani, G.; Lever, M.; Yan, J.; Mesner, D.; Robinson, C. V.; Dushek, O.; van der Merwe, P. A.; Howarth, M., SpyAvidin Hubs Enable Precise and Ultrastable Orthogonal Nanoassembly. *J. Am. Chem. Soc.* **2014**, *136* (35), 12355-12363.
- 37. Gu, Y.; Zhao, J.; Johnson, J. A., A (Macro)Molecular-Level Understanding of Polymer Network Topology. *Trends Chem.* **2019**, *1* (3), 318-334.
- 38. Knoff, D. S.; Szczublewski, H.; Altamirano, D.; Fajardo Cortes, K. A.; Kim, M., Cytoskeleton-Inspired Artificial Protein Design to Enhance Polymer Network Elasticity. *Macromolecules* **2020**, *53* (9), 3464-3471.
- 39. Sengupta, D.; Heilshorn, S. C., Protein-Engineered Biomaterials: Highly Tunable Tissue Engineering Scaffolds. *Tissue Eng.*, *Part B* **2010**, *16* (3), 285-293.
- 40. Xue, B.; Tang, D.; Wu, X.; Xu, Z.; Gu, J.; Han, Y.; Zhu, Z.; Qin, M.; Zou, X.; Wang, W.; Cao, Y., Engineering hydrogels with homogeneous mechanical properties for controlling stem cell lineage specification. *Proc. Natl. Acad. Sci. U. S. A.* **2021**, *118* (37), e2110961118.
- 41. Ray, T. R.; Choi, J.; Bandodkar, A. J.; Krishnan, S.; Gutruf, P.; Tian, L.; Ghaffari, R.; Rogers, J. A., Bio-Integrated Wearable Systems: A Comprehensive Review. *Chem. Rev.* **2019**, *119* (8), 5461-5533.
- 42. Sano, T.; Cantor, C. R., Streptavidin-containing chimeric proteins: design and production. *Methods Enzymol.* **2000**, *326*, 305-11.

- 43. Meyer, D. E.; Chilkoti, A., Purification of recombinant proteins by fusion with thermally-responsive polypeptides. *Nat. Biotechnol.* **1999,** *17* (11), 1112-1115.
- 44. Camp, C. P.; Peterson, I. L.; Knoff, D. S.; Melcher, L. G.; Maxwell, C. J.; Cohen, A. T.; Wertheimer, A. M.; Kim, M., Non-cytotoxic Dityrosine Photocrosslinked Polymeric Materials With Targeted Elastic Moduli. *Front. Chem.* **2020**, *8*, 173.
- 45. Jacobsen, M. T.; Fairhead, M.; Fogelstrand, P.; Howarth, M., Amine Landscaping to Maximize Protein-Dye Fluorescence and Ultrastable Protein-Ligand Interaction. *Cell Chem. Biol.* **2017**, *24* (8), 1040-1047.e4.
- 46. Pähler, A.; Hendrickson, W. A.; Kolks, M. A.; Argaraña, C. E.; Cantor, C. R., Characterization and crystallization of core streptavidin. *J. Biol. Chem.* **1987**, *262* (29), 13933-13937.
- 47. Kurzban, G. P.; Bayer, E. A.; Wilchek, M.; Horowitz, P. M., The quaternary structure of streptavidin in urea. *J. Biol. Chem.* **1991**, *266* (22), 14470-14477.
- 48. Lin, T.-S.; Wang, R.; Johnson, J. A.; Olsen, B. D., Topological Structure of Networks Formed from Symmetric Four-Arm Precursors. *Macromolecules* **2018**, *51* (3), 1224-1231.
- 49. Zakeri, B.; Fierer, J. O.; Celik, E.; Chittock, E. C.; Schwarz-Linek, U.; Moy, V. T.; Howarth, M., Peptide tag forming a rapid covalent bond to a protein, through engineering a bacterial adhesin. *Proc. Natl. Acad. Sci. U. S. A.* **2012**, *109* (12), E690-E697.
- 50. Gao, X.; Fang, J.; Xue, B.; Fu, L.; Li, H., Engineering Protein Hydrogels Using SpyCatcher-SpyTag Chemistry. *Biomacromolecules* **2016**, *17* (9), 2812-2819.
- 51. Gu, Y.; Kawamoto, K.; Zhong, M.; Chen, M.; Hore, M. J. A.; Jordan, A. M.; Korley, L. T. J.; Olsen, B. D.; Johnson, J. A., Semibatch monomer addition as a general method to tune and enhance the mechanics of polymer networks via loop-defect control. *Proc. Natl. Acad. Sci. U. S. A.* **2017**, *114* (19), 4875-4880.
- 52. Rubinstein, M.; Dobrynin, A. V., Associations leading to formation of reversible networks and gels. *Curr. Opin. Colloid Interface Sci.* **1999**, *4* (1), 83-87.
- 53. Tang, S.; Wang, M.; Olsen, B. D., Anomalous Self-Diffusion and Sticky Rouse Dynamics in Associative Protein Hydrogels. *J. Am. Chem. Soc.* **2015**, *137* (11), 3946-3957.
- 54. Rapp, P. B.; Omar, A. K.; Silverman, B. R.; Wang, Z.-G.; Tirrell, D. A., Mechanisms of Diffusion in Associative Polymer Networks: Evidence for Chain Hopping. *J. Am. Chem. Soc.* **2018**, *140* (43), 14185-14194.
- 55. Walton, T. A.; Rees, D. C., Structure and stability of the C-terminal helical bundle of the E. coli mechanosensitive channel of large conductance. *Protein Sci.* **2013**, *22* (11), 1592-1601.
- 56. MacEwan, S. R.; Chilkoti, A., Elastin-like polypeptides: Biomedical applications of tunable biopolymers. *Pept. Sci.* **2010**, *94* (1), 60-77.

- 57. Zhang, Y.-N.; Avery, R. K.; Vallmajo-Martin, Q.; Assmann, A.; Vegh, A.; Memic, A.; Olsen, B. D.; Annabi, N.; Khademhosseini, A., A Highly Elastic and Rapidly Crosslinkable Elastin-Like Polypeptide-Based Hydrogel for Biomedical Applications. *Adv. Funct. Mater.* **2015**, *25* (30), 4814-4826.
- Lust, S. T.; Hoogland, D.; Norman, M. D. A.; Kerins, C.; Omar, J.; Jowett, G. M.; Yu, T. T. L.; Yan, Z.; Xu, J. Z.; Marciano, D.; da Silva, R. M. P.; Dreiss, C. A.; Lamata, P.; Shipley, R. J.; Gentleman, E., Selectively Cross-Linked Tetra-PEG Hydrogels Provide Control over Mechanical Strength with Minimal Impact on Diffusivity. ACS Biomater. Sci. Eng. 2021, 7 (9), 4293-4304.
- 59. Lutolf, M. P.; Hubbell, J. A., Synthesis and Physicochemical Characterization of End-Linked Poly(ethylene glycol)-co-peptide Hydrogels Formed by Michael-Type Addition. *Biomacromolecules* **2003**, *4* (3), 713-722.
- 60. Shih, H.; Lin, C.-C., Cross-Linking and Degradation of Step-Growth Hydrogels Formed by Thiol–Ene Photoclick Chemistry. *Biomacromolecules* **2012**, *13* (7), 2003-2012.
- 61. Yang, J.; Jacobsen, M. T.; Pan, H.; Kopeček, J., Synthesis and Characterization of Enzymatically Degradable PEG-Based Peptide-Containing Hydrogels. *Macromol. Biosci.* **2010**, *10* (4), 445-454.

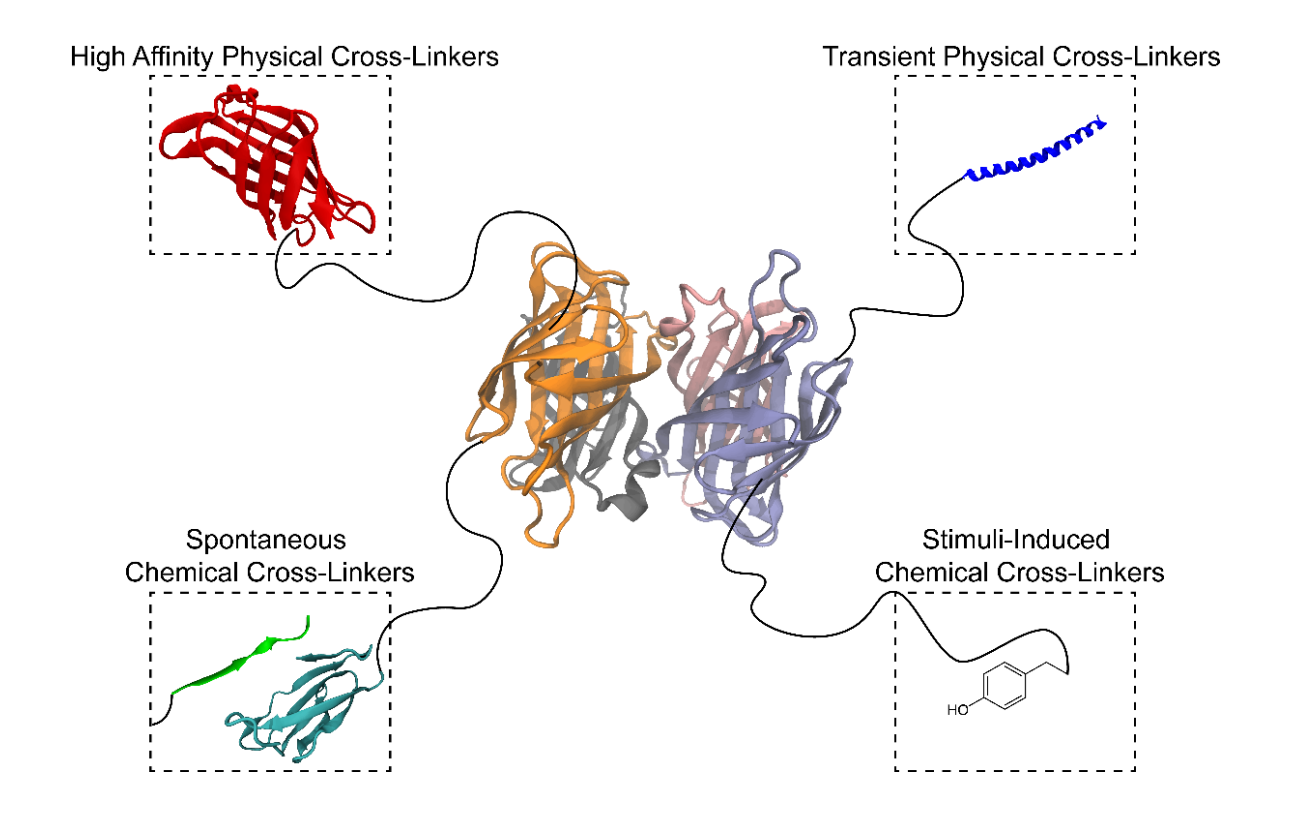


Figure 1. Schematic of the four-arm streptavidin precursors and second-level self-assembly building blocks for developing bottom-up design strategies that fabricate specific and stable protein-network materials. Streptavidin homotetramer (PDB: 1SWE) with customizable secondary cross-linking methods to control the mechanics of hydrogel fabrication. Secondary cross-linkers are illustrated together, attached to the same streptavidin cross-linker by a flexible protein strand, but were tested separately in this study to identify optimal mechanisms for the assembly of protein-network materials. Secondary cross-linkers, include a SAv monomer (SAv; red), coiled-coil protein monomer (P; blue; PDB: 1MZ9), SpyTag-SpyCatcher system (Spy; cyan and green; PDB: 4MLI), and tyrosine residue (Y) for photo-cross-linking. These results in artificial proteins of SAv-flexible protein-SAv, P-flexible protein-SAv, Spy-flexible protein-SAv, and Y-flexible protein-SAv.

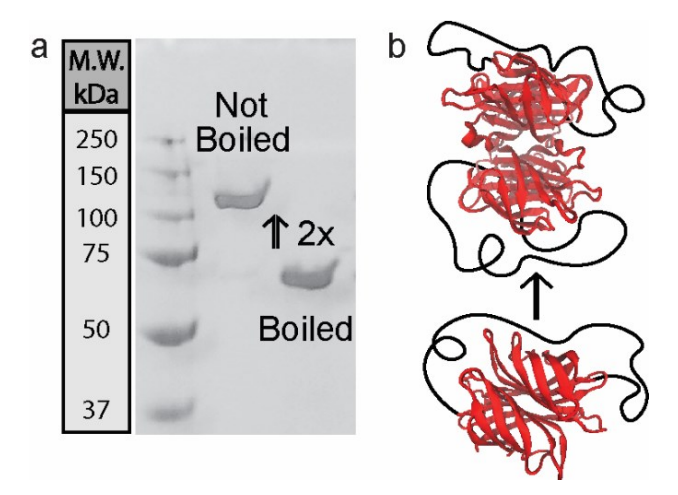


Figure 2. Analysis of SAv-C₂₄-SAv homotetramerization. (a) SDS-PAGE analysis of SAv-C₂₄-SAv self-association. (b) Schematic demonstrating the self-looping of an individual SAv-C₂₄-SAv protein, followed by the molecular self-assembly of two self-looped SAv-C₂₄-SAv proteins into a tetramer.

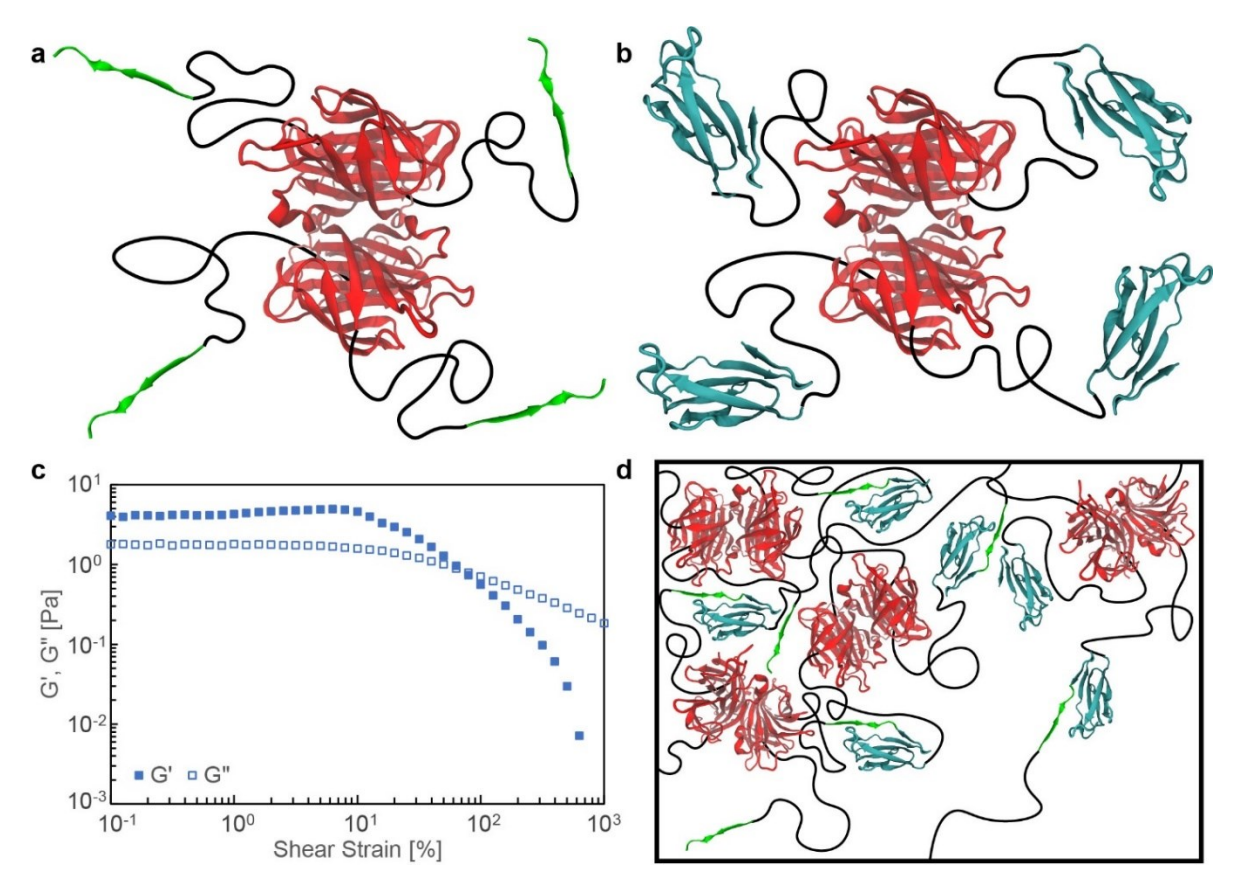


Figure 3. Spy-C₂₄-SAv protein hydrogels and their rheological characterization. (a,b) Schematics of a SpyTag-C₂₄-SAv four-arm precursor and a SpyCatcher-C₂₄-SAv four-arm precursor. (c) Representative strain sweep of a Spy-C₂₄-SAv hydrogel at a constant 10 rad/s angular frequency. Spy denotes that the linkage of SpyTag and SpyCatcher. (d) Illustration demonstrating the inhomogeneous protein-network formation of Spy-C₂₄-SAv.

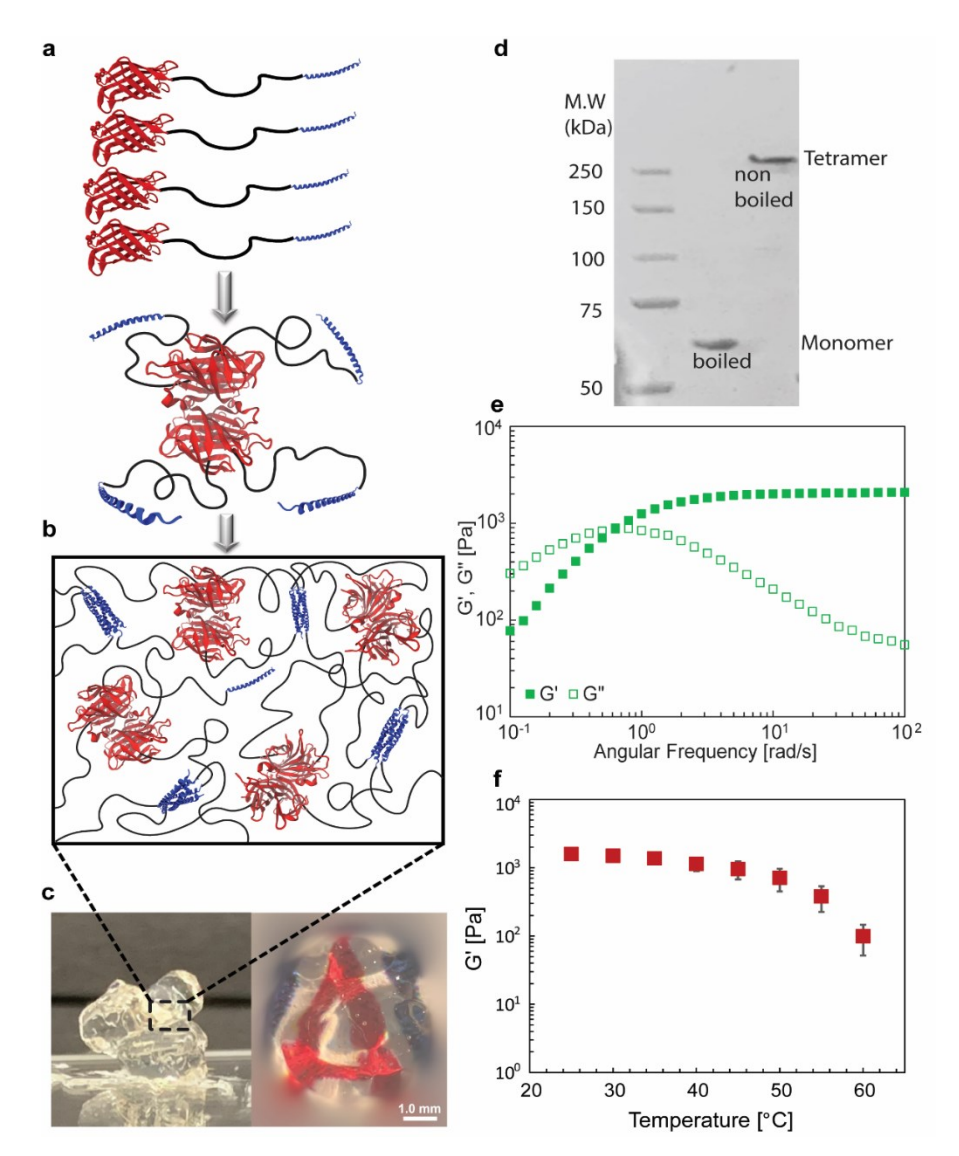


Figure 4. Characterization of SAv-based hydrogels with secondary, transient cross-linkers. (a) Schematic of a P-C24-SAv four-arm precursor from the molecular self-assembly of P-C₂₄-SAv monomers. (b) Illustration demonstrating the protein-network formation of P-C24-SAv after the second molecular self-assembly of P coiled-coil cross-linkers. (c) Pictures of self-standing hydrogel and hydrogel under the light microscope. (d) SDS-PAGE analysis of boiled and non-boiled P-C24-SAv proteins. See the molecular weight of P-C24-SAv monomers, measured by liquid chromatography-mass spectroscopy (LC-MS) in Figure S3. (e) Representative frequency sweep of a P-C24-SAv hydrogel at a constant 1% strain. (f) Temperature sweep of P-C24-SAv hydrogels from 25 to 60 °C at a constant 10 rad/s frequency and 1% strain (*N*=3; mean ± standard error).

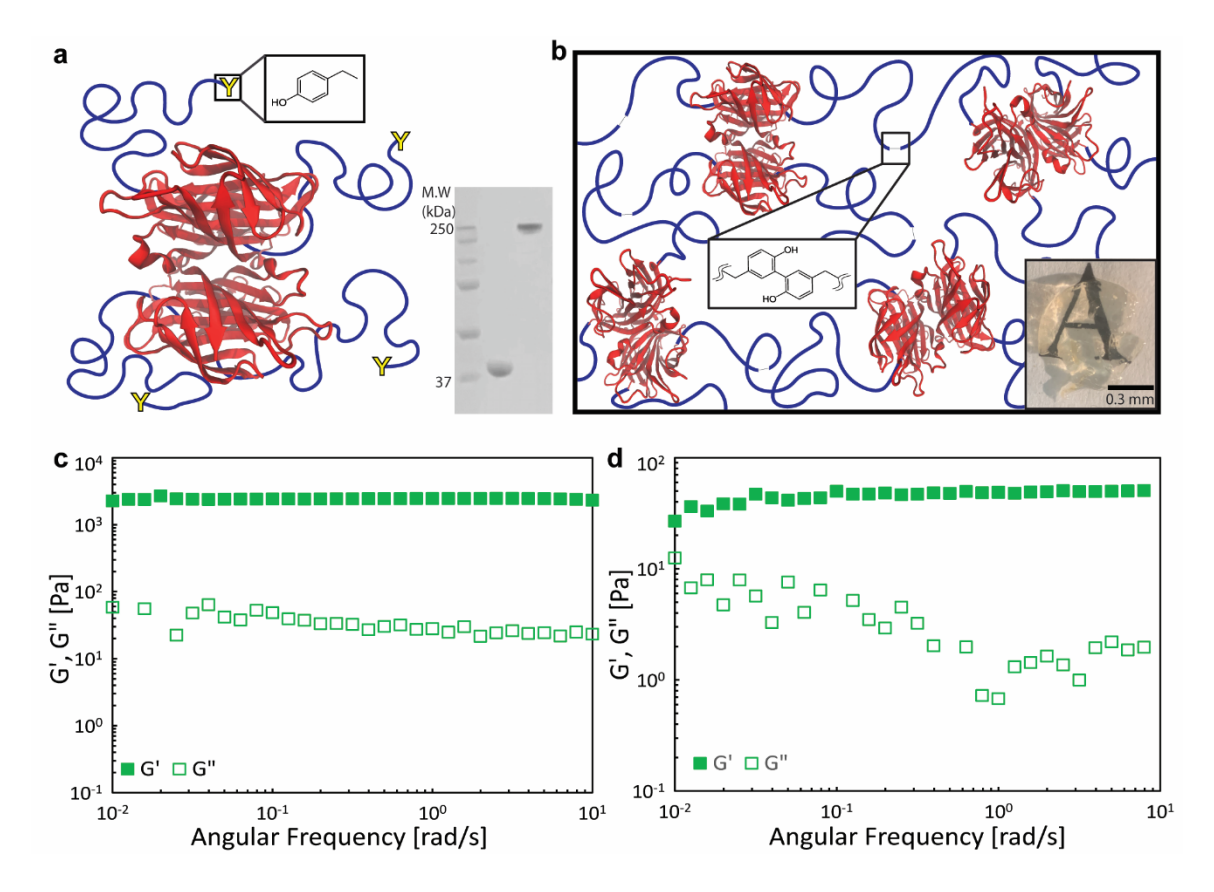


Figure 5. Mechanical stability of SAv-based hydrogels with secondary, photo-induced chemical cross-linkers using rheological characterization. (a) Tyr-ELP-SAv four-arm precursor with SDS-PAGE that shows the monomer and tetramer of the protein when boiled (middle lane) and non-boiled (right lane), respectively. (b) Illustration and hydrogel image demonstrating the protein-network of Tyr-ELP-SAv due to the formation of dityrosine covalent bonds and SAv tetramer self-assembly. (c,d) Representative frequency sweep of a Tyr-ELP-SAv hydrogel at a constant 1% strain. The proteins were photo-cross-linked with 250 μ M ruthenium and 80 mM ammonium persulfate (c) and with 31 μ M ruthenium and 15 mM ammonium persulfate (d).

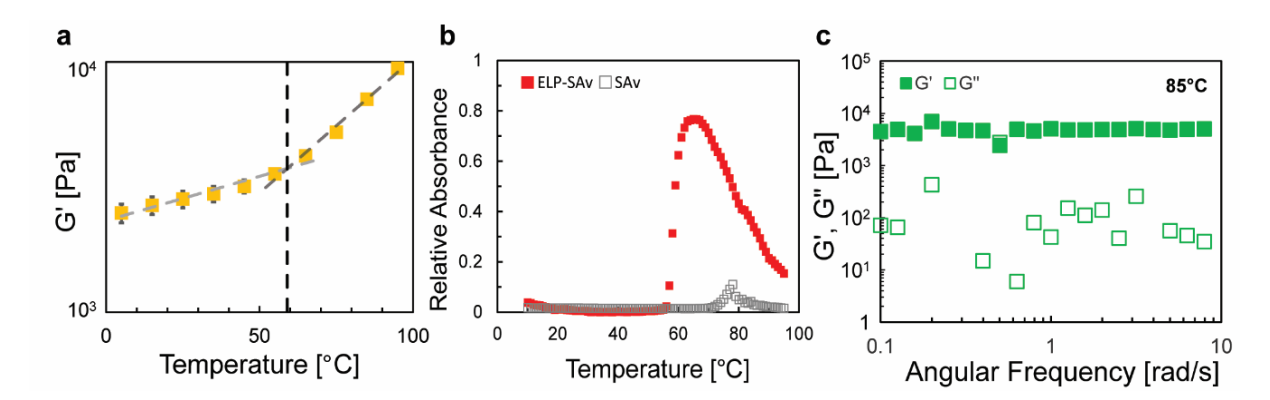


Figure 6. Thermal stability of tetra-SAv in protein-network hydrogels. (a) Temperature sweep rheology experiments on A₂YA₂-A₄₈-SAv hydrogels with a constant 10 rad/s frequency and 1% strain. Trendlines were made from 5 to 55 °C (light gray dashed line) and from 65 to 95 °C (dark gray dashed line). Black dashed line represents the intersection. (b) UV-Vis measurement (at 350 nm) of A₂YA₂-A₄₈-SAv proteins and SAv proteins as a control in the temperature ranges from 10 to 95 °C. UV-Vis data of SAv in the wide range of wavelength at 25 °C is in Figure S1. (c) Representative frequency sweep data of A₂YA₂-A₄₈-SAv hydrogel at 85 °C and a constant 1% strain.